DOI: 10.1021/cg1005538

CRYSTAL GROWTH & DESIGN Article

2010, Vol. 10
4428–4432

Single Crystal Growth and Characterization of Superconducting LiFeAs

Igor Morozov,[†,‡] Alexander Boltalin,[‡] Olga Volkova,[‡] Alexander Vasiliev,[‡] Olga Kataeva,[†,#] Ulrike Stockert,[†] Mahmoud Abdel-Hafiez,[†] Dirk Bombor,[†] Anne Bachmann,[†] Luminita Harnagea,[†] Madeleine Fuchs,[†] Hans-Joachim Grafe,[†] Günter Behr,[†] Rüdiger Klingeler,[†,§] Sergey Borisenko,[†] Christian Hess,[†] Sabine Wurmehl,*[,†] and Bernd Büchner[†]

[†]*Leibniz Institute for Solid State and Materials Research, D-01171 Dresden, Germany,* [‡]*Moscow State University, Moscow 119991 Russia,* [#]*A. E. Arbuzov Institute of Organic and Physical Chemistry, Russian Academy of Science, Russia, and* [§]*Kirchhoff Institute for Physics, D-69120 Heidelberg, Germany*

Received April 26, 2010; Revised Manuscript Received August 20, 2010

ABSTRACT: Large and high quality single crystals of the new unconventional superconductor LiFeAs were grown by a new approach using the self-flux technique. Both energy dispersive X-ray spectroscopy and inductively coupled plasma mass spectroscopy revealed a stoichiometric Li/Fe/As composition. Measurements of the magnetic susceptibility reveal the superconducting transition at $T_C = 17$ K with a very sharp ΔT_C and a 100% shielding fraction and, thus, bulk superconductivity. This sharp transition is also found by measurements of the specific heat and by measurements of the temperature dependence of the resistivity. Nuclear quadrupole resonance (NQR) spectroscopy reveals a very sharp resonance line, with a much smaller line width than reported for all other FeAs superconductors, confirming the high ordering of the LiFeAs single crystals also on a local scale.

Introduction

The research on ternary and quaternary compounds containing FeAs antifluorite-type layers has brought new inspiration to the community striving for high-T_C superconductivity. Despite the fact that at ambient pressure the highest critical temperature in iron-based superconductors (e.g., 55 K in SmFeAs(O,F)[1]) is still low compared to that of copper-oxide superconductors (135 K in $HgBa_2Ca_2Cu_3O_x$[2]), their sensitivity to chemical substitutions and pressure makes iron arsenides rather promising objects to study. By now, three distinct series of pnictide superconductors are known, namely, the 1111 series (ROFeAs and AeFFeAs),[3,4] the 122 series ($AeFe_2As_2$ and AFe_2As_2),[5,6] and the 111 series (AFeAs)[7] with R = rare-earth element, A = alkaline metal, and Ae = alkaline-earth metal. All series have the structural $Fe_2As_2^{2-}$ component in common (see, for example, ref 8). LiFeAs crystallizes in a tetragonal Cu_2Sb/PbClF-type structure (*P*4/*nmm*) and consists of Fe_2As_2 layers connected by edge-sharing $FeAs_4$ tetrahedra, similar to other pnictide superconductors.

A structural transition, for example, from the tetragonal to an orthorhombic structural phase, as observed for the parental 1111 and 122 compounds, has not yet been observed in LiFeAs, even with applying pressure up to 20 GPa.[9] Within the undoped, parental 1111 and 122 compounds, the Fe ions tend to form magnetically ordered states and participate in building up a high density of states at the Fermi level.[10] Upon appropriate doping, the antiferromagnetic phase or, alternatively, the spin density wave phase is suppressed. The superconducting phase appears around optimal doping close to or overlapping with the magnetic phase. Therefore, magnetic ordering is considered to be a prerequisite for iron arsenides to become superconducting.[11−13]

Among the parental phases of the new FeAs superconductors the 111 series, including LiFeAs and NaFeAs, remains the least investigated even though their structural simplicity might simplify their study. In particular, this series addresses an important question concerning the role of magnetism in the formation of a superconducting state in iron arsenides.[14] No indication of magnetic ordering was seen in measurements of various physical properties of polycrystalline or very small single crystalline LiFeAs samples.[7,14,15] In contrast, clear evidence on the coexisting superconductivity and magnetism was obtained in similar measurements on NaFeAs single crystals.[16] Recent studies using neutrons seem to indicate LiFeAs to be a weakly coupled single-gap superconductor.[17] In order to provide a perfect playground for the meaningful comparison of the physical properties of LiFeAs and in particular to study the superconducting gap, for example, by means of angle-resolved photoemission spectroscopy (ARPES), high quality single crystals are required.

There are several ways to grow crystals of Fe-based superconductors. For example, growth from Sn flux has the disadvantage of the possible incorporation of Sn into the structure of the pnictide superconductors which affects their properties.[18] Tapp et al.[7] were the first to succeed in the growth of LiFeAs single crystals. The authors have grown small crystals by a solid-state reaction using stoichiometric quantities of Li, Fe, and As. Wang et al. reported on the synthesis of LiFeAs using high pressure yielding polycrystalline samples which are nearly phase pure and might exhibit a small off-stoichiometry.[15] Two different ways of preparing polycrystalline LiFeAs were proposed by Pitcher et al., starting either from Li and prereacted FeAs or from Li_3As, Fe, and FeAs.[19] Tiny single crystals, a few tenths of a millimeter in size, were obtained by prolonged annealing at low temperature by Chu et al.[14] Crystals with a size of $6 \times 6 \times 3$ mm^3 were recently obtained by the Bridgman method.[20] However, the

*To whom correspondence should be addressed E-mail: s.wurmehl@ifw-dresden.de.

 Published on Web 09/16/2010

resistivity curves of the Bridgman crystals might indicate a foreign phase and a complete diamagnetic shielding is not unambiguously deduced from the magnetization data.[20] Here, we report on self-flux technique yielding larger single crystals of LiFeAs than previously reported[7,14,20] with a very high quality and their comprehensive characterization.

Experimental Methods

Crystal Growth, Morphology, and Stoichiometry. Powder materials of Fe (Alfa Aesar, 99.99%), As (Alfa Aesar, 99.99%) and lumps of Li (Alfa Aesar, 99.9%) were used. An optimized self-flux technique was developed in order to overcome the difficulties in crystal growth and limited sample quality of LiFeAs. Our crystal growth approach is described as follows. All preparation steps were performed in an argon box to take into account the high sensitivity to moisture of both Li and the resulting LiFeAs. For the self-flux growth, an optimized molar ratio of the elements Li/Fe/As = 3:2:3 was used. First, a mixture of As and Fe was prepared by thoroughly grinding in an agate mortar and to ensure homogeneity. Small lumps of the Li metal were added to the Fe−As mixture, which was then placed into an Al_2O_3 ceramic crucible. The crucible was inserted into a Nb container, covered by a Nb cap with outlets for the flux (therefore, working as a sieve). The Nb crucible was welded in Ar atmosphere with a base pressure of 1.5 atm, and the sealed Nb container was enclosed in a quartz ampule under lowered Ar pressure (0.25 atm) to prevent any oxidation. The sample was heated up to 1363 K for 18 h, then kept at this temperature for another 5 h and cooled down to 873 K with a rate of 4.5 K/h. At this temperature, the ampule was turned over to remove the liquid flux and left in a furnace for an additional 6 h. Finally, the ampule was extracted from the furnace and cooled in air. After the quartz ampule was unsealed in an argon box, it was confirmed that no leakage of liquid flux occurred. Evidently, complete crystallization occurs in the system above 873 K. The thin LiFeAs plates formed associates separated by relatively mild and brittle flux. The individual single crystals with lateral dimensions of $(12 \pm 6) \times (12 \pm 6) \times (0.3 \pm 0.05)$ mm^3 were chipped off from the associates mechanically.

Microstructure, crystal perfection, and the Fe:As ratio were examined by scanning electron microscopy (SEM, XL30 Philipps, IN400) equipped with an electron microprobe analyzer for semiquantitative elemental analysis using the energy-dispersive X-ray (EDX) mode. Inductively coupled plasma mass spectroscopy (ICP MS, Agilent 7500C Quadrupole ICP-MS with dynamic reaction cell) was used to confirm the 1:1:1 composition of LiFeAs. For ICP MS analysis, about 20 mg of the LiFeAs single crystal was dissolved in a leak-free glass ampule in 900 mg of nitric acid (concentration 63%). Complete dissolution was ensured by stirring for 4 h. The resulting solution was diluted with deionized water up to 50 mL. A calibration curve was taken using standard reference solutions of Li, Fe and As. The reference standard solutions of Li, Fe and As were prepared by consecutive diluting an initial solution with a concentration of 10 mg/L (High Purity Standards, Charleston, USA). The measured concentrations are 173.0 mg/L (Fe), 232.4 mg/L (As), and 21.2 mg/L (Li). The relative standard deviation of the measured concentration is about 5%. For comparison, e.g. with the NQR data, we also prepared polycrystalline LiFeAs samples in a Nb crucible by reacting Li, Fe, and As at 1060 K for 48 h.

Single Crystal X-ray Diffraction. A thin plate of $0.17 \times 0.06 \times 0.02$ mm^3 was cut from a larger LiFeAs single crystal. The crystal was immediately put in Fomblin oil to avoid contact with air, mounted on a MiTiGen cryo loop, and placed in a cooled nitrogen gas stream on a Bruker AXS Kappa APEX II CCD sealed tube diffractometer with graphite-monochromated MoK_α-radiation (λ = 0.71073 Å). The data were collected using the complete sphere mode at 100 K with ω and ϕ scans ($\pm h$, $\pm k$, $\pm l$), $[(\sin\theta)/\lambda] = 0.70$ Å^{-1}. The following programs were used: data collection *APEX2* program,[21] data reduction *SAINT*,[22] absorption correction *SADABS* program,[23] structure solution *SHELXS97*,[24] and structure refinement by full-matrix least-squares against F^2 using *SHELXL-97*.[24]

Nuclear Quadrupole Resonance spectroscopy. Nuclear quadrupole resonance (NQR) spectroscopy was measured using a commercial Tecmag Apollo spectrometer. A copper coil was wrapped around the crystal (9 mg, dimensions $3.3 \times 2.9 \times 0.3$ mm^3), and both crystal and coil were sealed in a quartz tube in Argon atmosphere to avoid any contact of the crystal with air.

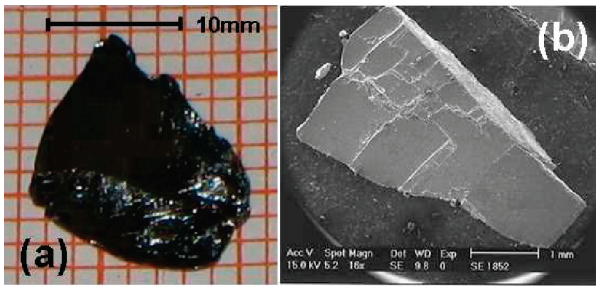

Figure 1. Optical image of a LiFeAs crystal with a shiny and metallic-like surface (a) and a SEM picture (b).

Physical Properties. Measurements of the magnetic properties were made using a Quantum Design VSM SQUID magnetometer. The dimensions of the sample were $a = 2.1 \pm 0.1$ mm, $b = 1.8 \pm 0.1$ mm, $c = 0.2 \pm 0.1$ mm. The specific heat as a function of temperature was obtained by a relaxation technique using a Quantum Design PPMS. The temperature dependence of the electrical resistivity was measured on samples with lateral dimensions of 2.57 mm × 0.39 mm × 0.30 mm using a standard 4-probe DC technique. The electrical contacts were made inside a glovebox under Argon atmosphere. Angle-resolved photoemission spectroscopy (ARPES) has been performed using the synchrotron radiation of the BESSY storage ring.[25]

Results and Discussion

Crystal Growth, Morphology, and Stoichiometry. The crystals obtained from the growth procedure as described above are fragile and prone to exfoliation. They cleave along the *ab* plane and in particular between two layers of Li.[25] This offers very clean, equivalent, and neutral surfaces for all surface sensitive techniques (e.g., ARPES). The crystals are highly sensitive to air moisture, which complicates both the growth and the study of the single crystals. Figure 1a shows an optical image of such a crystal, demonstrating the large size of about $(12 \pm 6) \times (12 \pm 6) \times (0.3 \pm 0.05)$ mm^3 and the shiny and metallic-like surface.

Figure 1b shows an SEM picture of a LiFeAs single crystal. Evidently, the surface morphology of the samples shows terrace-like features on the flat surface, originating from the layer-by-layer growth mechanism of the crystals. Similar terraces were seen on the surface of $Ae_{1-x}K_xFe_2As_2$ (Ae = Ba, Sr) single crystals grown in Sn flux.[26,27] The layer-by-layer growth also reflects the layered morphology of the LiFeAs structure, consisting of (FeAs) and Li planes. The bonding between the adjacent FeAs layers, mediated via As−Li−As bonds, is weaker compared to the bonding within the FeAs layers. This causes a faster growth rate within the *ab* layers, while the growth along the *c* axis is slow, leading to the formation of thin and platelet-like crystals. In our growth experiment, the crystals grow from bottom to the top of the crucible, indicating a directional solidification.

EDX analysis of the composition indicated the Fe/As molar ratio as 1:1, as expected. This technique does not provide a measure of the Li content in the sample, as EDX is not reliable in the quantification of light elements. The stoichiometry of LiFeAs is an important issue, as Li-deficient samples have been reported to exhibit changed electrical conductivity.[15]

ICP MS offers the advantage over EDX to measure the stoichiometric composition of light elements. From this data, the molar ratio Li/Fe/As is found to be 0.99:1.00:1.00, consistent with a stoichiometric LiFeAs composition. ARPES

Table 1. Crystal Data for LiFeAs Single Crystal Diffractometry at 100 K

temperature	100 K
space group	*P*4/*nmm* (No. 129)
a (Å^3)	3.7678(4)
c (Å^3)	6.3151(8)
V (Å^3)	89.65(2)
Z	2
ρ_{calc} (g cm^{-3})	5.101
μ (mm^{-1})	26.129
multiscan absorption correction	$0.095 \leq T \leq 0.623$
θ range	3.23−30.06
collected reflections	1243
independent reflections	101 (R_{int} = 0.029)
observed reflections	96 $I \geq 2\sigma(I)$
R	0.017
wR^2	0.047
max residual electron density (e Å^{-3})	1.02
min residual electron density (e Å^{-3})	−0.61
goodness-of-fit	1.20

Table 2. Atomic Positions and Thermal Parameters for LiFeAs at 100 K

atom	Wyckoff site	x	y	z	U_{eq} (e Å^2)
Li	2*c*	0.2500	0.2500	0.655(2)	0.014(2)
Fe	2*a*	−0.2500	0.2500	0.0000	0.0071(3)
As	2*c*	0.2500	0.2500	0.23626(9)	0.0069(2)

measurements performed on a LiFeAs single crystal from the same batch were found to be in agreement with an almost exact stoichiometry.[25]

Structural Characterization. Single Crystal X-ray Diffraction. LiFeAs crystallizes in the tetragonal Cu_2Sb/PbClF structure type in the space group *P*4/*nmm* (No. 129). The results of the structural refinement of the single crystal diffractometry data at 100 K are summarized in Table 1. Table 2 gives the atomic positions and thermal parameters for LiFeAs at 100 K.

Our X-ray data have a very low R value, in particular compared to previous reports,[7,15,19] indicating very good agreement between the data and the refinement parameters.

The quality of our refinement is also reflected by the absence of rest electron density peaks and a good internal consistency of the experimental data.

Nuclear Quadrupole Resonance Spectroscopy. Nuclear quadrupole resonance (NQR) probes the electric-field gradient (EFG) at the position of the nucleus, which strongly depends on the local environment. NQR is thus able to reveal the local ordering, and small deviations from a homogeneous charge distribution or lattice anomalies such as deficiencies or defects which will lead to a broadening of the NQR line or to splitting into several lines. Figure 2 shows the ^{75}As NQR spectrum of a LiFeAs single crystal at room temperature. The resonance line can be well fitted to a Gaussian distribution which gives a line width (FWHM) of 64 kHz only (see Figure 2). Such a small line width is exceptional for iron arsenides and confirms the high quality and electronic homogeneity of our LiFeAs single crystals. For comparison, undoped LaOFeAs has a line width of 220 kHz,[28,29] and the undoped $CaFe_2As_2$ has a FWHM of 480 kHz.[30] On doping, these FWHM's increase considerably. Figure 2 also compares the NQR spectrum taken from a LiFeAs polycrystal. The polycrystal exhibits a broader width of 113 kHz, which is about two times broader than the line width of the single crystal. Moreover, the small line width excludes deficiencies and antisite disorder, as observed in LiFeAs by Pitcher et al.[19] Thus, the NQR measurement also demonstrates the excellent structural ordering in the LiFeAs single crystals on a local scale.

Physical Properties. Magnetic Susceptibility and Specific Heat. Figure 3a shows the magnetic susceptibility of LiFeAs,

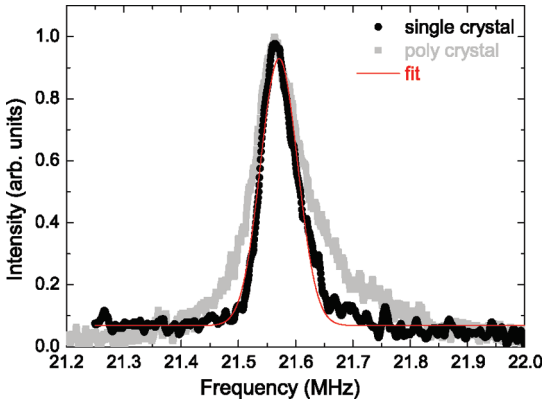

Figure 2. ^{75}As NQR resonance line of the single crystal at room temperature. Gray data points correspond to data taken in the polycrystalline sample. The solid line is a Gaussian fit.

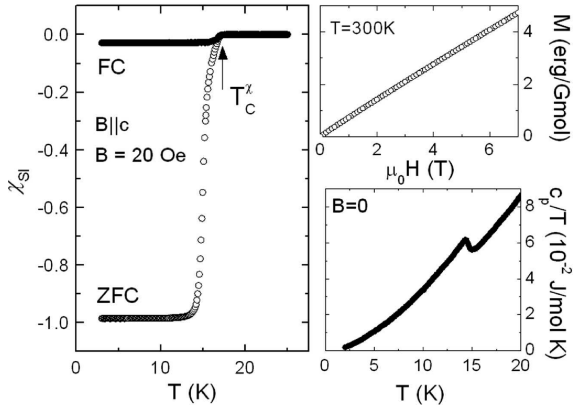

Figure 3. Measurements of the magnetic susceptibility of LiFeAs, measured with both zero-field cooling (zfc) and field cooling (fc) (a), magnetization as a function of magnetic field at 300 K (b), and measurement of the specific heat (c).

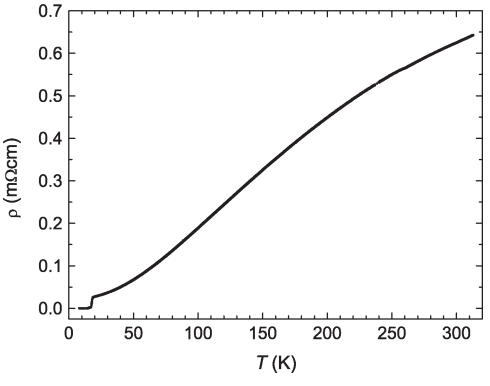

Figure 4. Resistivity as a function of temperature of a LiFeAs single crystal.

measured with both zero field cooling (zfc) and field cooling (fc) with the magnetic field of 20 Oe applied parallel to the c axis. The onset value of T_C is 17 K (Figure 3a). The magnetization data have been corrected for demagnetization effects by an ellipsoid approximation based on the lateral dimensions of the samples.[31] The magnetic susceptibility (zfc) shows a complete diamagnetic shielding, thus confirming bulk superconductivity in our LiFeAs single crystal. The magnetization as a function of magnetic field at 300 K (Figure 3) shows a linear dependence,

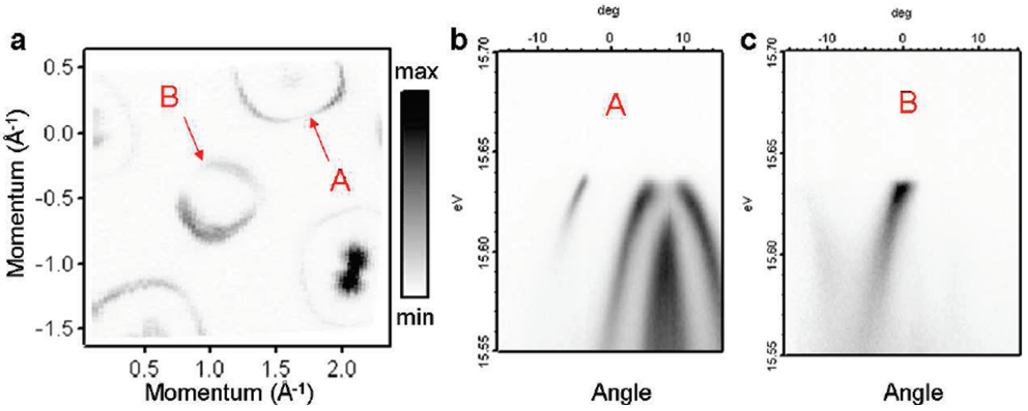

Figure 5. Fermi surface of LiFeAs taken using 70 eV photons (a). Momentum-energy cuts A and B through the k-space indicated in panel (a) by the arrows (photon energy 20 eV) (b, c).

which proves a pure paramagnetic behavior and the absence of any magnetic impurities, such as Fe_2O_3, Fe_3O_4, or FeAs. To be specific, by comparison with the magnetization of bulk γ-Fe_2O_3 and Fe_3O_4, respectively, our data exclude phase fractions of more than 10^{-4} for both compositions.

The superconducting transition was also followed by measurements of the specific heat revealing a very sharp transition (Figure 3). This further confirms the quality of our crystals. Details of the data analysis will be discussed elsewhere.[32]

Resistivity. Figure 4 shows the in-plane resistivity of a LiFeAs crystal as a function of temperature, which in the normal-state resembles that of optimally doped La1111.[33,34] The onset of superconductivity is observed at $T_C^{onset} = 18.8 \pm 0.4$ K, and the transition temperature for 90% and 10% of the normal state is $T_C^{90\%} = 18.3\ K \pm 0.5$ K and $T_C^{10\%} = 17.1\ K \pm 0.5$ K, respectively, in line with the transition temperatures obtained by measurements of the susceptibility. The transition width is defined as $[T(90\%) - T(10\%)]$, yielding a very sharp transition width ΔT_C of 1.2 K. The residual resistivity, which in general originates from scattering at defects and impurities, is 0.025 mΩ cm. Thus, the very low residual resistivity further confirms the high quality of our LiFeAs crystals. We mention that, in samples contacted in air (not shown here), we observed a modified resistivity behavior in particular at high temperature and a higher residual resistivity similar to the resistivity curves observed by others.[7,15,20]

Angle-Resolved Photoemission Spectroscopy. Angle-resolved photoemission spectroscopy (ARPES) has been performed to study the electronic structure of our single crystals. The results of the ARPES study corroborate the stoichiometric composition of our LiFeAs single crystals and the absence of variations of the Li content within different crystals. LiFeAs cleaves between two layers of Li,[25] which provides clean, equivalent, and neutral surface layers to investigate. The high quality of our crystals enabled the observation of the Fermi surface (Figure 5a) and well-defined quasiparticles in a broad momentum space region (Figure 5b,c). We have found a strong renormalization of the bandwidth by a factor of 3 as well as a high density of states at the Fermi level caused by the presence of a Van Hove singularity at the Gamma-point. The latter seems to be an indispensable condition for the superconductivity in LiFeAs to occur (for details see ref 25).

Conclusion

For the first time, large LiFeAs crystals were grown using a self-flux technique. The high quality of our large LiFeAs single crystals was shown by several methods. The superconducting transition occurs ~17 K with a very sharp ΔT_C and bulk superconductivity. We observed no indication of a magnetic transition, giving no evidence to the coexistence of superconductivity and magnetism even in LiFeAs single crystals. The size and quality of our crystals will open new routes to study the properties, and in particular the electronic structure, of LiFeAs.

Acknowledgment. The authors thank M. Deutschmann, S. Pichl, K. Leger, and S. Gass for technical support and M. A. Bolshov and I. Ph. Seregina for help with the ICP MS analysis. I. M. acknowledges support from the Ministry of Science and Education of Russian Federation under State contract P-279 and by RFBR-DFG (Project No. 10-03-91334). O.K. acknowledges funding by DFG Grant KN240/15-1. Work was supported by the DFG program FOR 538 and the priority program SPP 1458 with the projects GR3330/2 and BE1749/13. The authors thank A. Holcombe (Ohio State University) for proofreading.

Supporting Information Available: Powder pattern data; X-ray crystallographic information file (CIF) for the crystal diffractometry data at 100 K. This material is available free of charge via the Internet at http://pubs.acs.org/.

References

(1) Ren, Z. A.; Lu, W.; Yang, J.; Yi, W.; Shen, X.-L.; Li, Z.-C; Che, G.-C; Dong, X.-L.; Sun, L.-L.; Zhou, R; Zhao, Z.-X. *Chin. Phys. Lett.* **2008**, *25*, 2215.
(2) Gao, L.; Xue, Y. Y.; Chen, R; Xiong, Q.; Meng, R. L.; Ramirez, D.; Chu, C. W.; Eg-gert, J. H.; Mao, H. K. *Phys. Rev. B* **1994**, *50*, 4260.
(3) Kamihara, Y; Watanabe, T.; Hirano, M.; Hosono, H. *J. Am. Chem. Soc.* **2008**, *130*, 3296.
(4) Tegel, M.; Johansson, S.; Weiss, V.; Schellenberg, I.; Hermes, W.; Pottgen, R.; Johrendt, D. *Europhys. Lett.* **2008**, *84*, 67007.
(5) Rotter, M.; Tegel, M.; Johrendt, D. *Phys. Rev. Lett.* **2008**, *101*, 107006.
(6) Sasmal, K.; Lv, B.; Lorenz, B.; Guloy, A. M.; Chen, R; Xue, Y-Y; Chu, C.-W. *Phys. Rev. Lett.* **2008**, *101*, 107007.
(7) Tapp, J. H.; Tang, Z.; Lv, B.; Sasmal, K.; Lorenz, B.; Chu, P. C. W.; Guloy, A. M. *Phys. Rev. B* **2008**, *78*, 060505.
(8) Day, C. *Phys. Today* **2009**, *62*, 36.
(9) Zhang, S. J.; Wang, X. C; Sammynaiken, R.; Tse, J. S.; Yang, L. X.; Li, Z.; Liu, Q. Q.; Desgreniers, S.; Yao, Y; Liu, H. Z.; Jin, C. Q. *Phys. Rev. B* **2009**, *80*, 014506.
(10) Dong, J.; Zhang, H. J.; Xu, G.; Li, Z.; Li, G.; Hu, W Z.; Wu, D.; Chen, G. R; Dai, X.; Luo, J. L.; Fang, Z.; Wang, N. L. *Europhys. Lett.* **2008**, *83*, 27006.
(11) Luetkens, H.; et al. *Nat. Mater.* **2009**, *8*, 305.
(12) Drew, A. J.; et al. *Nat. Mater.* **2009**, *8*, 310.

(13) Chu, J.-H.; Analytis, J. G.; Kucharczyk, C; Fisher, I. R. *Phys. Rev. B* **2009**, *014506*, 79.
(14) Chu, C. W.; Chen, R; Gooch, M.; Guloy, A. M.; Lorenz, B.; Lv, B.; Sasmal, K.; Tang, Z.; J.H., T.; Xue, Y. *Physica C: Supercond.* **2009**, *469*, 326.
(15) Wang, X. C; Liu, Q. Q.; Ly, Y. X.; Gao, W. B.; Yang, L. X.; Yu, R. C; Li, F. Y.; Jin, C. Q. *Solid State Commun.* **2008**, *148*, 538.
(16) Chen, G. R; Hu, W. Z.; Luo, J. L.; Wang, N. L. *Phys. Rev. Lett.* **2009**, *102*, 227004.
(17) Inosov, D. S. et al. *Phys. Rev. Lett.* **2010**, *104*, 187001.
(18) Su, Y.; Link, P.; Schneidewind, A.; Wolf, T.; Adelmann, P.; Xiao, Y.; Meven, M.; Mit-tal, R.; Rotter, M.; Johrendt, D.; Brueckel, T.; Loewenhaupt, M. *Phys. Rev. B* **2009**, *79*, 064504.
(19) Pitcher, M. J.; Parker, D. R.; Adamson, P.; Herkelrath, S. J. C; Boothroyd, A. T.; Ibber-son, R. M.; Brunelli, M.; Clarke, S. J. *Chem. Commun.* **2008**, *2008*, 5918.
(20) Song, Y J.; Ghim, J. S.; Min, B. H.; Kwon, Y S.; Jung, M. H.; Rhyee, J.-S. arXiv: 1002.2249 **2010**.
(21) *Bruker APEX2*; Analytical X-ray Instruments Inc.: Madison, Wisconsin, USA, 2008.
(22) *Bruker SAINT*; Analytical X-ray Instruments Inc.: Madison, Wisconsin, USA, 2008.
(23) Sheldrick, G. M.; *SADABS: Empirical Absorption and Correction Software*; University of Gottingen, Institut fur Anorganische Chemie der Universitat: Gottingen, Germany, 2008.
(24) Sheldrick, G. *Acta Crystallogr.* **2008**, *A64*, 112.
(25) Borisenko, S. V.; Zabolotnyy, V. B.; Evtushinsky, D. V.; Kim, T. K.; Morozov, I. V.; Yaresko, A. N.; Kordyuk, A. A.; Behr, G.; Vasiliev, A.; Follath, R.; Biichner, B.*Phys. Rev. Lett.* **2010**, *105*, 067002.
(26) Karpinski, J.; et al. *Physica C* **2009**, *469*, 370.
(27) Sun, G. L.; Sun, D. L.; Konuma, M.; Popovich, P.; Boris, A.; Peng, J. B.; Choi, K.-Y; Lemmens, P.; Lin, C. T. arXiv:0901.2728 **2010**.
(28) Grafe, H. J.; Lang, G.; Hammerath, R; Paar, D.; Manthey, K.; Koch, K.; Rosner, H.; Curro, N. J.; Behr, G.; Werner, J.; Leps, N.; Klingeler, R.; Buchner, B. *New J. Phys.* **2009**, *11*, 035002.
(29) Lang, G.; Grafe, H. J.; Paar, D.; Hammerath, R; Manthey, K.; Behr, G.; Werner, J.; Buchner, B. *Phys. Rev. Lett.* **2010**, *104*, 097001.
(30) Curro, N. J.; Dioguardi, A. P.; ApRoberts-Warren, N.; Shockley, A. C; Klavins, P. *New J. Phys.* **2009**, *11*, 075004.
(31) Osborne, J. A. *Phys. Rev.* **1945**, *67*, 351.
(32) Stockert, U.; Wolter, A. U. B.; Klingeler, R.; Abdel-Hafiez, M.; Mozorov, I.; Wurmehl, S.; Behr, G.; Buchner, B., in preparation **2010**.
(33) Hess, C; Kondrat, A.; Narduzzo, A.; Hamann-Borrero, J. E.; Klingeler, R.; Werner, J.; Behr, G.; Buchner, B. *Europhys. Lett.* **2009**, *87*, 17005.
(34) Kondrat, A.; Hamann-Borrero, J. E.; Leps, N.; Kosmala, M.; Schumann, O.; Kohler, A.; Werner, J.; Behr, G.; Braden, M.; Klingeler, R.; Buchner, B.; Hess, C. *Eur. Phys. J. B* **2009**, *70*, 461.